



HAL
open science

Revealing the Potential of Waste Fibers from Timber Production and Clearings for the Development of Local Bio-based Insulation Fiberboards in French Guiana

Julie Bossu, Jérôme Moreau, Christine Delisée, Nicolas Le Moigne, Stéphane Corn, Rodolphe Sonnier, Amandine Viretto, Jacques Beauchene, Bruno Clair

► To cite this version:

Julie Bossu, Jérôme Moreau, Christine Delisée, Nicolas Le Moigne, Stéphane Corn, et al.. Revealing the Potential of Waste Fibers from Timber Production and Clearings for the Development of Local Bio-based Insulation Fiberboards in French Guiana. *Waste and Biomass Valorization*, 2023, 14, pp.4281-4295. 10.1007/s12649-023-02085-9 . hal-03848251v2

HAL Id: hal-03848251

<https://hal.science/hal-03848251v2>

Submitted on 4 Apr 2023

HAL is a multi-disciplinary open access archive for the deposit and dissemination of scientific research documents, whether they are published or not. The documents may come from teaching and research institutions in France or abroad, or from public or private research centers.

L'archive ouverte pluridisciplinaire **HAL**, est destinée au dépôt et à la diffusion de documents scientifiques de niveau recherche, publiés ou non, émanant des établissements d'enseignement et de recherche français ou étrangers, des laboratoires publics ou privés.

Revealing the Potential of Waste Fibers from Timber Production and Clearings for the Development of Local Bio-based Insulation Fiberboards in French Guiana

Julie Bossu¹ · Jérôme Moreau^{2,3} · Christine Delisée³ · Nicolas Le Moigne⁶ · Stéphane Corn⁷ · Rodolphe Sonnier⁶ · Amandine Viretto⁵ · Jacques Beauchêne⁴ · Bruno Clair⁸

✉ Julie Bossu
julie.bossu@cnrs.fr

¹ EcoFoG, CNRS, Kourou, Guyane, France

² Limbha, Ecole Supérieure du Bois, Nantes, France

³ Département GCE, I2M, Bordeaux, France

⁴ Ecofog, CIRAD, Guadeloupe, France

⁵ BioWooEB, Univ. Montpellier, CIRAD, Montpellier, France

⁶ Polymers Composites and Hybrids (PCH), IMT Mines Ales, Ales, France

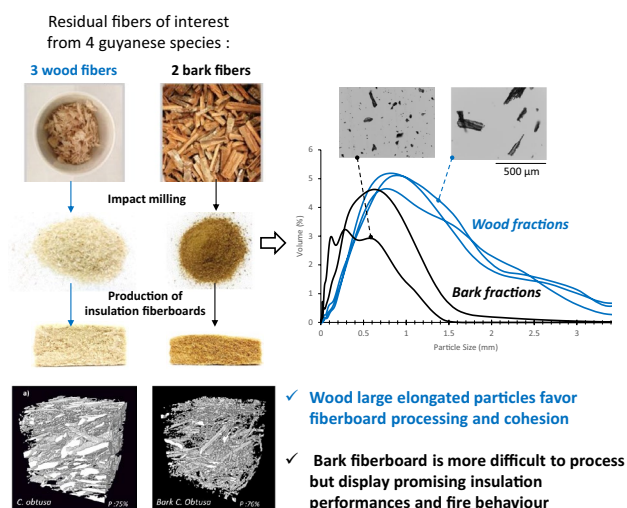
⁷ LMGC, IMT Mines Ales, Univ Montpellier, CNRS, Ales, France

⁸ LMGC, Montpellier, France

Abstract

In French Guiana, the development of bio-circular value chains to convert residual biomass into insulation fiberboard represents a promising opportunity for energy-efficient construction. The objectives of this work are to identify and characterize resources of interest and discuss the relationships between fiber properties, manufacturing parameters, and fiberboard performance. Five wood and bark fibers were fractionated from residual biomass of 4 local species, and their fractions analyzed by: laser granulometry, thermal gravimetric analysis (TGA), and pyrolysis combustion flow calorimetry (PCFC). Fiberboards were produced using a thermomechanical process and their microstructure, thermal, and sorption properties were characterized by X-ray tomography, hot plate technique, and dynamic vapor sorption (DVS). Morphological analysis showed that large and elongated wood fractions form thick and cohesive fibrous networks, while small-sized bark fractions are more difficult to process, requiring more compaction and synthetic fiber additives due to lower natural self-adhesion. Despite processing difficulties, bark fiberboards showed the best insulation performance, comparable to commercial reference products. TGA and PCFC tests revealed that bark fibers have better thermal stability and fire behavior compared to wood, and a stronger water affinity compared to wood fractions, highlighting the need for further investigations of durability performance in tropical conditions in the long term, but also a potential interest for humidity regulation.

Graphical Abstract



Keywords Tropical biomass valorization · Residual fibers · Bio-circular economy · Insulation fiberboards · Microstructure · Thermal properties

Statement of Novelty

This work constitutes the first attempt to explore the potential of residual biomass in the production of insulation fiberboard in French Guiana, in alignment with local objectives of developing sustainable constructive solutions adapted to tropical regions. The interdisciplinary experimental strategy developed here is innovative and opens discussions on the relationships between fiber morphology, fiberboard microstructure, and end-use performance. The outcomes of this work will help drive the selection of new resources to be considered for fiberboard production in French Guiana, and help identify the key processing parameters to be tested. Our results highlight two promising residual fibers for fiberboard production, evidencing similar to better insulation properties than those reported for commercial reference products. This work is a starting point for future research projects.

Introduction

French Guiana is located in the hot and humid Amazon region. To provide comfortable living conditions, construction methods and materials must guarantee good solar protection and humidity regulation. Traditionally, buildings in French Guiana have been designed using passive architectural strategies including building orientation, daylighting, natural ventilation, and solar energy, and have been built with durable wood elements. Today, because of demographic growth (by 2027, around 6600 new houses need to be built per year, according to the regional environment, planning and housing agencies, DEAL [1]) the vernacular style has been progressively replaced by large-scale construction of less expensive and poorly ventilated houses. Furthermore, the use of air-conditioning to cool and dry interiors has become widespread, accounting for a large share of domestic energy consumption. The development of efficient and affordable biomaterials would support an ecological transition towards more energy efficient buildings and sustainable housing. Today, most of the insulating products used in French Guiana are imported. Made from non-renewable resources and with high transportation costs, they are also poorly adapted to high-moisture and high-temperature conditions. For example: hydrophobic mineral wools collapse under the weight of water which accumulates on surface fibers as a result of local condensation effects, creating thermal bridges; reflective insulation boards can become less efficient when the metallic surfaces peel off due to high temperature. These traditional materials are also inefficient regarding

humidity regulation. Using locally sourced wood fibers to produce high-performance insulating materials would help meet long term regional sustainable construction objectives [2]. Natural fibers have several benefits compared to conventional mineral and synthetic fibers: low density, good specific mechanical properties, non-abrasive properties, low acoustic and thermal conductivity, biodegradability, and high hydric inertia [3, 4].

The non-woven process appears to be a promising technological solution for the manufacturing of insulation fiberboards. In this technique, adapted from the textile industry, a thermo-mechanical process ensures the cohesion of the fiber mat by the interlocking of fibers through carding [5], requiring no prior addition of glue. Manufactured using light industrial equipment, and only a small proportion of synthetic fibers, this industry could easily be developed in French Guiana. To avoid further exploitation of the Amazonian rainforest, residual biomass is the preferred locally available fiber resource. There are abundant high quality waste wood fibers from the exploitation of local species, selected for high technical performance, in timber production. In addition to the abundant residues from commercially exploited species, small-sized trees of fast-growing species frequently cut during clearings have also been selected for study in this work. The methodology used in this study is easily transferable to other tropical regions where similar wood residues and fast-growing species are found.

There are several knowledge gaps for the development of such materials:

The Quality of the Tropical Species in this Study has Never Been Evaluated at Fiber Scale

It is difficult to predict the quality of the fractions obtainable from milling. The selected wood and bark specimens have different anatomical microstructures (cells type, shape, and organization), densities, and chemical compositions, which should influence the final particle size distribution and the morphology of the fractions after milling. Furthermore, the thermal properties and flammability of these materials is unknown.

The Manufacturing Process of Fiberboards has Never Been Adapted to Tropical Resources

Unlike wood fibers from temperate species, and mostly soft-wood species [6], tropical wood and bark fibers, characterized by different structures and morphology, have never been tested. Fiberboard processing parameters may need to be optimized for the specificities of tropical resources.

The Relationships Between fiber Characteristics and Fiberboard Properties are Poorly Understood

Since no glue was used during the production of the fiberboards, thermal conductivity was expected to depend on the intrinsic properties of the fibers and the resulting microstructure and porosity distribution within the fiber mat [7]. This raises questions concerning the importance of parameters to be taken into account when selecting fibers for the production of insulation fiberboards: What are the effects of fiber morphological features on the microstructure and porosity of fiberboards? Is the microstructure of the fibers, or their intrinsic insulating properties, more important?

The specific goals of the present study were therefore: (i) to characterize the morphological and thermal properties of the selected tropical waste fibers and fractions obtained after milling; (ii) to optimize the production process for each resource; (iii) to investigate microstructure-properties relationships; (iv) to evaluate the insulation performance and water affinity of the fiberboards produced; and (v) to propose processing improvements.

This work constitutes, to our knowledge, the first attempt to study the thermal properties of waste fibers from French Guiana and their suitability for the production of insulation fiberboards.

Material and Methods

Selection of Resources

Of 1800 identified tree species in French Guiana, about 60 are of commercial interest, among which *Dicorynia guianensis* Amshoff, Fabaceae (local name: Angélique; trade name: Basralocus), and *Sextonia rubra* (Mez.) Van der Werff, Lauraceae (local name: Grignon franc; trade name: Louro vermelho) represent around 68% of the overall volume harvested over the period 2010–2021 (*Centre Technique des Bois et de la Forêt de Guyane, CTBFG, (2021), unpublished raw data*). These two commercial species have thus been selected as a promising source of industrial waste fibers, as the French National Forest Office (ONF) foresees a 20% increase in total log harvesting between 2021 and 2025 compared to the 2010–2021 period, due to the increase in requirements for construction timber in response to local demographic growth. Consequently, the annual volume of available sawmill by-products will also increase and will be easy to source, as 5 sawmills account for 94% of annual timber production, limiting logistics costs.

Another resource of interest is the bark and wood of small trees of fast-growing species, not suitable for timber

production. Future land use changes, in particular the creation of an additional 45,000 ha of agricultural land by 2030, in alignment with local government objectives,¹ will generate large volumes of otherwise unusable woody biomass. Two abundant fast-growing species have been selected for study: *Cecropia obtusa* Trécul., Cecropiaceae (local name *Bois canon*), the most abundant tree in anthropized areas of French Guiana, also harvested for the extraction of the high-value chemical compounds found in its bark; and *Virola surinamensis*, (Rol. Ex Rottb.) Warb., Myristicaceae (local name *Yayamadou*; trade name: *Virola*) the bark of which has well-defined fiber bundles [8], expected to be easily isolated by defibration.

Although the species we have cited are commonly found throughout the Amazon basin, none of these resources is currently commercially valued.

For testing, one heartwood board was collected at the Kourou sawmill for both of the commercial wood species *Dicorynia guianensis* Amsh. (*D. guianensis*) and *Sextonia rubra* (Mez) van der Werff (*S. rubra*). One young specimen (5 m height, approximately 2 years-old) was harvested in a secondary forest near the Paracou experimental station (5°16'27N; 52°55'26W) for both of the fast-growing species *Cecropia obtusa* Trécul (*C. obtusa*; Bark *C. obtusa*) and *Virola surinamensis* (Rol. Ex Rottb.) Warb. (Bark *V. surinamensis*) to obtain wood and bark fibers. Bark was manually isolated and a radial plank was sawn at breast height. In order to obtain sufficient volume, more than 10 kg of material was collected for each resource. Samples were manually cut into chips with a knife and air-dried in the laboratory for one month.

Our final sampling thus consisted of 3 wood samples (*D. guianensis*, *S. rubra* and *C. obtusa*) and 2 bark samples (Bark *C. obtusa* and Bark *V. surinamensis*) (Fig. 1). The main characteristics of each wood species, based on past surveys on Guyanese wood properties [9, 10] are given in Table 1. No information could be found in the literature for the barks presented in this study.

Production and Characterization of Fibers

Production of Fibers

In previous studies on softwood, fiberboards were successfully manufactured from fibers with an average length of 1.6 mm [11]. To achieve these dimensions, we used an impact mill. This technology enables comminution of lignocellulosic materials while limiting energy consumption

¹ Data from the Regional Development Plan of French Guiana (SAR) of the Territorial Collectivity of French Guiana (CTG), approved by the decree of the Council of State n° 2016-931 of 6 July 2016.

Fig. 1 Sampling strategy. Wood fibers were collected from *D. guianensis*, *S. rubra* and *C. obtusa*. Bark fibers were collected from *C. obtusa* and *V. surinamensis*. Fibers were oven-dried at 60 °C for 3 days and milled into fine powder using an impact mil SM 300 (1.5 kg/h and 2000 rpm with 4 mm then 2 mm grid). Photos credits: *D. guianensis*: Romain Lehnebach; *S. rubra*: Emeline Houël; *C. obtusa*: Yves Caraglio; *V. surinamensis*: Inventaire National du Patrimoine Naturel

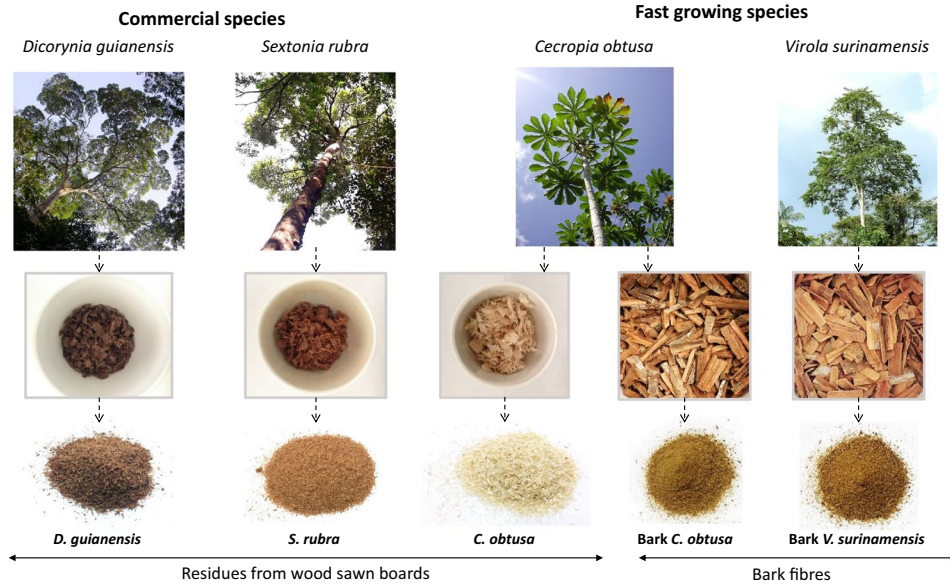


Table 1 Wood physical and chemical characteristics based on past surveys on Guyanese wood properties [9, 10]

Species	Physical properties			Biochemical composition				
	N	D12 (kg m ⁻³)	FSP (%)	N	Cellulose (%)	Lignin (%)	Extractives (%)	Ashes (%)
<i>D. guianensis</i>	90	790 (0.05)	28.6 (2.3)	7	45.5 (2.0)	35.9 (2.1)	4.4 (1.5)	0.7 (0.3)
<i>S. rubra</i>	28	660 (0.04)	29.4 (2.8)	3	47.8 (2.7)	31.7 (3.3)	9.1 (2.7)	0.4 (0.2)
<i>Cecropia sp.*</i>	6	320 (0.06)	40.7 (3.7)	2	52.5	23.3 (1.2)	4.8 (1.5)	1.2 (0.3)

N number of tested specimens, *D12* wood density at 12% RH, *FSP* Fiber Saturation Point. Standard deviation is given in brackets. Cellulose and lignin contents were measured by the K urschner and Klason methods respectively. Extractives were extracted in water. *Database reports measurement performed on *Cecropia* genus without specifying the studied species.

compared to thermo-mechanical or chemical methods [12]. Chips were oven-dried at 60 °C for 3 days to avoid caking during grinding, then fractionated into fine powder (Fig. 1) using an impact milling system (SM 300, Retsch) in continuous mode, at 1.5 kg/h and 2000 rpm. The chips were fractionated twice, first using a 4 mm grid, and second using a 2 mm grid. 5 kg of dry mass was produced for each resource.

Morphological Analysis

Morphological analysis was performed on the PLANET platform (technological platform specialized in the defibrating of lignocellulosic fibers, located at UMR IATE, Montpellier). The particle size distributions of the fractions were analyzed by laser diffraction using a laser granulometer (LS 13,320 XR, Beckman Coulter) in dry mode. Five replicates of 5 g per resource were tested, and showed good reproducibility. Particle size distribution is reported as percentiles denoted by the letter *d* followed by the % value. Thus, *d10*=*x* mm, *d50*=*y* mm, and *d90*=*z* mm means that 10%

of the sample is smaller than *x* mm, 50% is smaller than *y* mm, and 90% is smaller than *z* mm. Specific surface area (SSA) was also determined for each sample. SSA is a common measure applied to particulate solids like the fine fiber fractions studied in this work. The surface area per unit of mass is important during processing since many physical and chemical processes take place on the surface of solids.

A sample of each milled fraction was machine-sprayed onto a glass slide and analyzed using a particles shape analyzer (Morphologi 4, Malvern). This combines automated particle high-definition imaging with Raman spectroscopy to perform complex particle characterization. A mean of 47,727 particles were analyzed for each sample. Shape parameters like aspect ratio and circularity were detected using ‘sharp edge’ analysis.

Aspect ratio is defined as length divided by width. Circularity is a dimensionless value defined as the degree to which the particle is similar to a circle, taking into consideration the smoothness of the perimeter.

Thermal Gravimetric Analysis (TGA)

TGA was carried out to study the thermal behavior of the milled fibers during pyrolysis under oxygen flow using a Mettler TGA2 apparatus (Schwerzebbach, Switzerland) equipped with a XP5U balance. A 10 mg sample of each resource was heated from room temperature to 500 °C under air flow of 50 mL/min at a heating rate of 10 °C/min. Onset temperature (T_{onset}) was computed as the intersection point of the extrapolated baseline and the inflectional tangent at the beginning of the degradation peak. The peak degradation temperatures (T_{peak}) were taken at the maximum values of the mass-loss derivative curve. Analysis was done in duplicate for each sample with good reproducibility.

Pyrolysis Combustion Flow Calorimetry

Using a Fire Testing Technology microcalorimeter, A 2 (\pm 1) mg sample of each resource was heated under nitrogen flow to 750 °C at a heating rate of 1 °C/s. The released gases were mixed with oxygen (N_2/O_2 80/20) and burned in a combustion chamber at 900 °C to guarantee complete combustion. Heat release rate (HRR) was calculated from the oxygen consumption according to Hugg'tt's relation [23] (1 kg of consumed oxygen corresponds to 13.1 MJ of heat release). Each test was performed twice. The quantity of char, the peak of heat release rate (pHRR) and corresponding temperature ($T(\text{pHRR})$), the total heat release (THR), and the temperature of complete combustion (ΔH , calculated as the ratio between THR and mass loss) were determined.

Processing and Characterization of Fiberboards

Processing of Non-woven Fiberboards

Using a Laroche air-laid machine (Fig. 2), wood/bark fractions were carded using a rotating spiked roller (1100 to 2300 rpm), mixed with 6 mm-length synthetic bicomponent fibers (polyester/polypropylene, around 10% of the mass of the natural fibers), and blown (at 0.5 to 2 m/min) onto a vacuum perforated drum. Fibers in air-laid webs tend to



Fig. 2 Processing equipment used for 3D fiberboard formation: nap- opener or air-laid machine from Laroche

be isotropically oriented on the horizontal plane (but still random in-plane). Mat consistency was modulated by the stretching ratio (speed of entry delivery roller/speed of exit pressure rollers; adjustable from 0.5 to 2). Machine settings were adjusted in order to obtain a homogeneous fiber mat in mass and thickness (details of the machine parameters adjustments are provided in the results). The formed fiber mats were then superimposed to form a fiberboard. At this stage, fiberboard cohesion was provided only by the entanglement of fibers.

Non-woven Fiberboard Consolidation

In a Strahm hot-air oven (Fig. 3), the mats underwent 2 successive heating processes from 20 to 135 °C (melting temperature of the thermoplastic fiber sheath) at a rate of 60 °C/min, for 15 min, followed by a cooling to 20 °C at the same speed. This thermal dry bonding treatment capitalizes on the thermoplastic properties of synthetic fibers and results in very low density non-woven fibrous structures with good cohesion.

Characterization of Fiberboards

3D Microstructure

The internal microstructure of the fiberboards was imaged non-destructively, using a SkyScan X-ray microtomograph. A ϕ 9 mm by 10 mm cylindrical sample of fiberboard was X-rayed (tube voltage: 50 kV) and the signal recorded by 1.3 Mp CCD sensors coupled to scintillator by lens with 1:6 zoom range (1200 projections per scan, at 1000 ms). From the resulting 3D volume reconstruction of the sample, a subvolume was extracted from the grey level 3D images to remove borders and to avoid any boundary effects created either by cutting the sample or the X-Ray cone beam geometry. The pore sizes of wood/bark fibers were measured by performing successive openings of growing size on the virtual volume. The 3D images resolution was 6.9 microns/voxel and the analyzed volume was $5.5 \times 5.5 \times 5.5 \text{ mm}^3$. We used the SkyScan's volumetric NRecon reconstruction software for reconstruction and ImageJ software for analysis.

Insulation Properties

Insulation properties of the fiberboards were measured on $100 \times 100 \text{ mm}^2$ samples of varying thicknesses (depending on machine parameters, fiberboard thickness ranged from 15.2 to 30 mm for the different resources), stabilized at 20 °C and 65% RH). We conducted the hot plate technique using a Desprotherm device (Epsilon Alcen). A thermal source in the form of a thin heating mat (resistor) was placed between two samples of the material to be characterized. As the resistor was

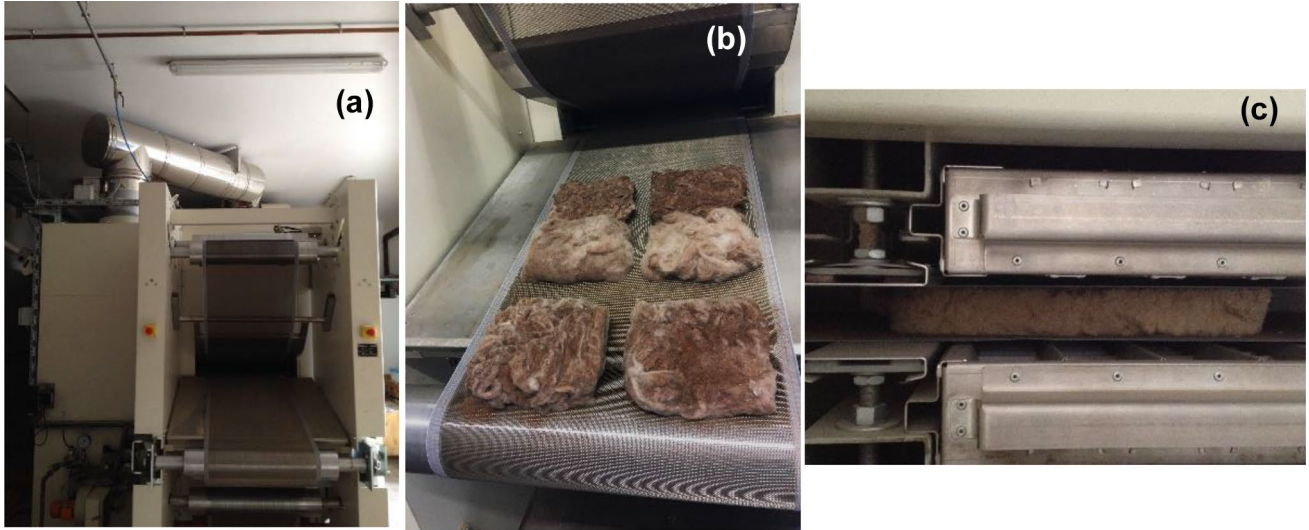


Fig. 3 Processing equipment used for insulation fiberboard consolidation: **a** Strahl hot-air oven, **b** fiberboard before entering the oven, **c** fiberboard being cooled in the oven

heated, the temperature evolution at the center of the resistor was measured with a thermocouple. The apparent thermal conductivity λ_{app}^* (W/m/K) of the material could be calculated by assessing its equivalent thermal effusivity b (W/K/m² s^{1/2}) and its bulk volumetric heat capacity $\rho^* \cdot C_p$ (W/m³/K¹), where ρ^* (kg/m³) is the bulk density and C_p (W/kg/K¹) is the specific heat capacity (Eq. 1). Tests were done in triplicate.

$$\lambda_{app}^* = \frac{b^2}{\rho^* \cdot C_p} \quad (1)$$

Dynamic Vapor Sorption (DVS)

Sorption was measured by dynamic vapor sorption (DVS) using a gravimetric sorption instrument (Service Solution Limited, UK, London). Two fiberboard specimens (10 ± 2 mg) were air-dried for two weeks. Mass change was constantly recorded under conditions of increasing RH (RH = 0%, 25%, 50%, 75% and 90%). Stabilized mass was recorded at a mass variation ratio dm/dt below 0.001%/min, and the moisture content (MC) was calculated. These conditions have been shown to be adequate for reaching constant mass uptake at each step of water vapor sorption for wood and biomaterials [13, 14]. The specific mass stabilization time (SMST_{75>90%RH}), was calculated as the time per mass unit necessary to reach equilibrium after a change in RH from 75 to 90% (Eq. 2).

$$SMST_{75>90\%RH} = \frac{\text{mass stabilization time from RH} = 75\% \text{ to } 90\%}{\text{Stabilized mass}_{RH=0\%}} \quad (2)$$

Results and Discussion

Morphological and Thermal Properties of Wood and Bark Fractions

Morphological Analysis

Morphological characterization of the milled fractions by laser granulometry revealed that most of the particles were much smaller than 2 mm (average d_{50} of 0.56 mm for all tested fractions) (Fig. 4). This aligns with the work of Mayer-Laigle et al. [12], David [15] and Rajaonarivony et al. [16], who obtained average particle sizes below 0.7 mm, for

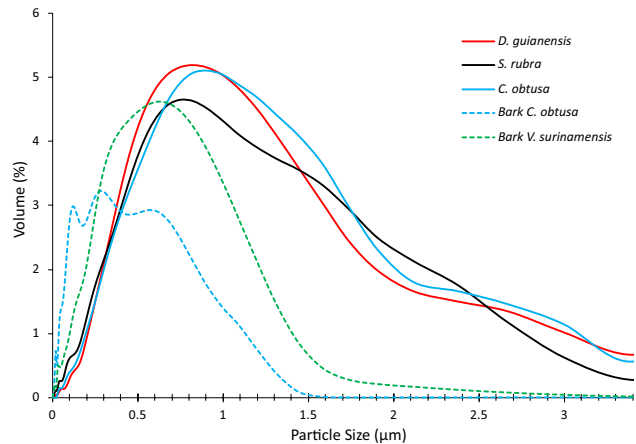


Fig. 4 Particle size distribution of the milled fractions for each tested material measured by laser granulometry (LS 13 320 XR, Beckman Coulter)

Table 2 Results of the morphological analysis of wood and bark fractions

Material	Laser diffraction					Particle imaging			
	N_1	d_{10} (mm)	d_{50} (mm)	d_{90} (mm)	SSA (cm ² /ml)	N_2	Aspect ratio	Circularity	CV%
<i>D. guianensis</i>	67,235	0.268	0.704	1.541	136.9	10,629	0.669	0.786	10.8
<i>S. rubra</i>	219,852	0.173	0.695	1.763	220.3	7500	0.559	0.601	3.4
<i>C. obtusa</i>	183,148	0.244	0.788	1.860	130.2	15,239	0.571	0.646	6.7
Bark <i>C. obtusa</i>	320,135	0.037	0.206	0.730	855.2	81,238	0.68	0.793	4.9
Bark <i>V. surinamensis</i>	118,443	0.083	0.424	1.008	503.5	135,352	0.702	0.833	3.4

N_1 mean number of detected elements for laser diffraction over the 5 replicates; particle size distribution percentiles, denoted by the letter d followed by the % value. Thus, $d_{10}=x$ μ m, $d_{50}=y$ μ m, and $d_{90}=z$ μ m means that 10% of the sample is smaller than x μ m, 50% is smaller than y μ m, and 90% is smaller than z μ m, N_2 mean number of detected elements for particle imaging; Aspect ratio, as length divided by width; Circularity, dimensionless value defined as the degree to which the particle is similar to a circle, CV% coefficient of variation.

wheat straw, vine shoots, and pine barks fibers, respectively, using a 2 mm grid and a similar milling protocol to the one used in this study.

Identical milling conditions resulted in fractions of variable size distributions depending on the species (Fig. 4 and Table 2). Size distributions of particles for milled wood specimens were similar ($d_{50}=0.73$ mm \pm 0.051 mm). Size distributions for milled bark specimens were both smaller, but were not similar ($d_{50}=0.42$ for *Bark V. surinamensis* and 0.21 mm for *Bark C. obtusa*). As samples were not sieved after milling, this resulted in a large amount of fine particles in bark specimens as illustrated in Fig. 4. Maharani et al. [17] showed that impact milling produces the highest proportion of particles under 0.3 mm (around 71.8% of the total volume) for 5 tropical tree species. We used a similar classification to sort the different fractions produced in this study (oversized particles > 0.7 mm; 0.7 mm < coarse particles < 0.3 mm; fine particles < 0.3 mm). The results obtained confirmed the existence of large amounts of fine particles in the bark specimens (up to 66.8% volume for *Bark C. obtusa* and 40.3% volume for *Bark V. surinamensis*) (Fig. 5), which could be the result of their specific anatomy or a lower resistance to impact milling compared to wood fibers.

Observations of air-sprayed fractions using a particle shape analyzer confirmed that wood samples contained longer particles compared to bark samples (Fig. 6). This method also allows a better characterization of the particle aspect ratio, and revealed that *S. rubra* and *C. obtusa* wood fractions had a larger share of elongated elements, while *D. guianensis* had smaller and more circular elements, but not as many as the bark fractions (Table 2).

The fractions produced are quite morphologically dissimilar, but representative of those which can be obtained using raw residual biomass from the wood industry sector, which is the focus of this study. However, the milling process could be optimized to obtain specific particle sizes. For example: by reducing drying intensity, fiber plasticity could be maintained and breakage during milling avoided

[12]; rotation speed and milling time could be reduced to limit fiber degradation; sieving could isolate specific particle sizes while maintaining satisfactory milling yields. Other fiber separation methods such as defibering require heavy technical installations ill-adapted to French Guiana for the foreseeable future.

We expect the heterogeneous morphological characteristics of the fractions described in this section to influence both the processing and the performance of the fiberboards. Specifically, while reduced fiber length may complicate fiberboard shaping, it has been found that fine particles promote microstructuration of the fiberboards and desirable thermal properties [18].

Thermal Analysis

All fractions resulting from milling were analyzed by thermal gravimetric analysis (TGA) to study their thermal decomposition kinetics (from room temperature to 600 °C at 10 °C/min, under oxygen flow), and using a Pyrolysis Combustion Flow Calorimeter (PCFC) (anaerobic pyrolysis and complete combustion) to characterize their flammability. Results are presented in Figs. 7 and 8 and the characteristic values are reported in Table 3.

In this work, the thermal degradation was studied under aerobic pyrolysis conditions. Compared to anaerobic pyrolysis, far fewer studies have been published on biomass combustion. Thermal degradation under oxidative atmosphere is more complex, considering that the presence of an oxidizing agent (air, oxygen, etc.) generates reactions between oxygen and solid reactants [19–21]. All fractions started losing weight at about 200 °C (i.e., 40 °C above the temperature used for fiberboards processing) and they all degraded in two stages: the first stage was rapid weight loss corresponding to pyrolysis or devolatilization (Stage I. Fig. 7); the second stage was weight loss corresponding to char oxidation due to the presence of oxygen (Stage II. Fig. 7) [22]. Under nitrogen flow, hemicellulose pyrolysis occurs around

Fig. 5 Representation of the particle size distribution of wood and bark powder samples over three-dimensional categories: oversized (OS) > 700 μm; coarse particle size (CPS): [300–700 μm]; fine particle size (FPS): [100–300 μm]

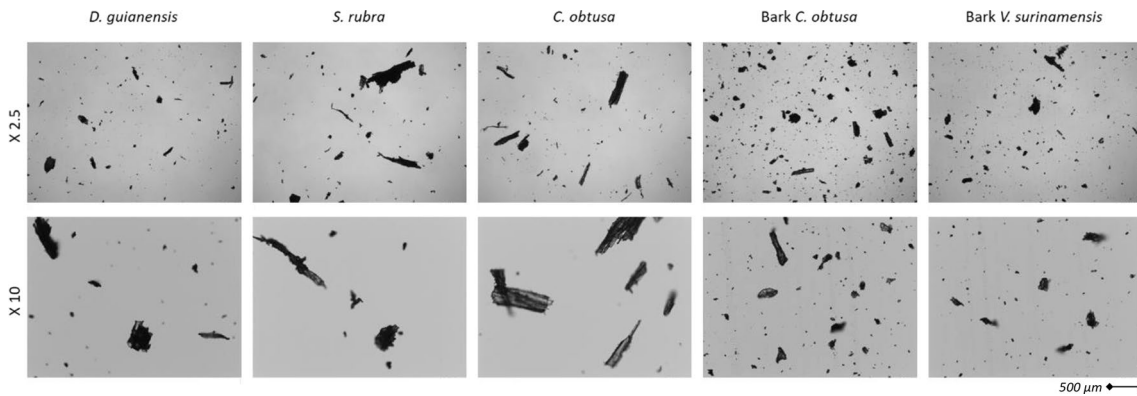
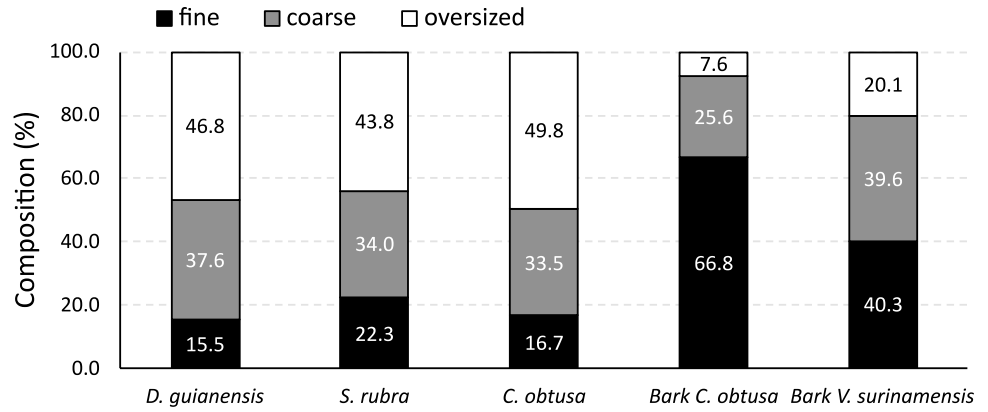


Fig. 6 Images of the milled fibers air-sprayed on a glass plate using a particles shape analyzer (Morphologi 4, Malvern)

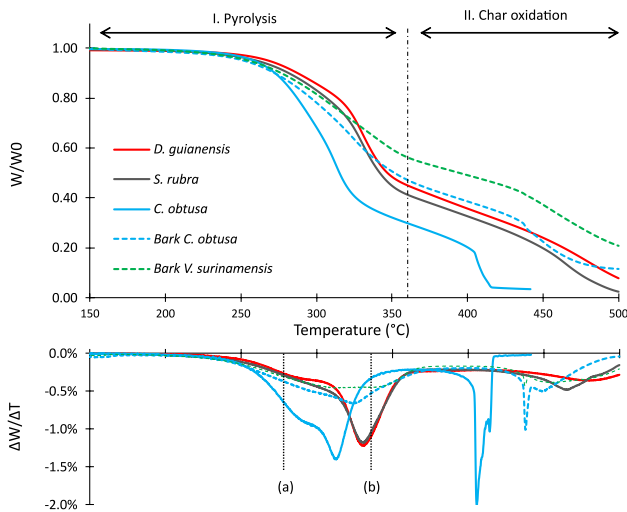


Fig. 7 Results of the thermal analysis (TGA) performed on the studied fractions. Mass variations (top) and its derivative (bottom) during heating under air flux at 10 °C/min up to 500 °C. Dotted lines (a) and (b) represent specific the specific degradation peaks of hemicelluloses and cellulose in oxidative conditions. Lignin degrades over a wider temperature range, from 350 to 450 °C

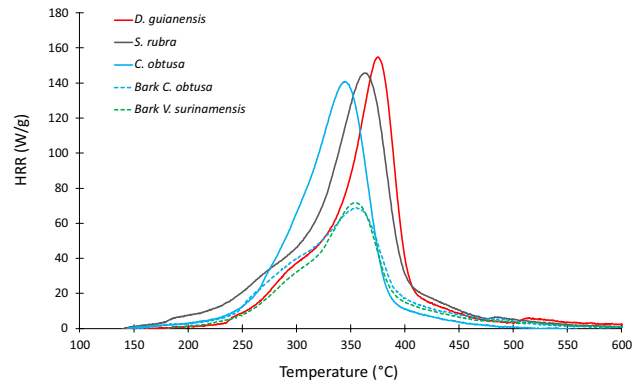


Fig. 8 Results of the PCFC tests conducted on the studied fractions. The evolution of the heat release rates (HRR) is shown as a function of the pyrolysis temperature

295 °C and cellulose pyrolysis occurs around 370 °C [23]. As lignin fractions have different stabilities, they decompose at a range of temperatures from 200 to 450 °C under nitrogen [24]. In the presence of oxygen, the devolatilization peaks appear at lower temperatures (– 15 °C for hemicellulose and – 35 °C for cellulose) [25] giving specific degradation

Table 3 Specific degradation temperatures determined by TGA thermograms and results from fire testing microcalorimeter measurements

	TGA measurements		Microcalorimeter measurements				
	T _{50%} (°C)	T _{peak} (°C)	Char (%)	pHRR (W/g)	T(pHRR) (°C)	THR (kJ/g)	ΔH (kJ/g)
<i>D. guianensis</i> wood	347	334; 481	18.32	154	372	11.1	13.5
<i>S. rubra</i>	342	332; 465	15.55	146	363.5	12.7	15.0
<i>C. obtusa</i>	314	313; 406	14.79	141	341	11.1	13.0
Bark <i>C. obtusa</i>	352	325; 438	25.24	67.5	354.5	7.1	9.4
Bark <i>V. surinamensis</i>	395	315; 438	24.83	74	354	7	9.3

peaks of hemicellulose and cellulose at 280 °C and 340 °C in aerobic conditions (peaks (a) and (b) on Fig. 7).

These values match the double peaks observed during pyrolysis of wood fractions *D. guianensis* and *S. rubra*. Both species showed similar behavior with almost identical cellulose degradation peaks (at 334 °C and 332 °C respectively, with identical intensity), likely because of their similar chemical composition (Table 1). Pyrolysis of hemicellulose and cellulose *C. obtusa* wood fractions was more pronounced, and the cellulose degradation peak appeared at a lower temperature (around 310 °C). This could be due to lower lignin content (around 23%, Table 1), lignin having been shown to decompose slowly during pyrolysis [26]. There was also a pronounced char oxidation peak at a lower temperature (406 °C), confirming its lower thermal stability compared to other samples. However, the combination of a low content of lignin with a high content of cellulose, as is the case for *C. obtusa*, might lead to charring and to incomplete combustion of these fibers, limiting their contribution to heat during burning.

The thermal stability of bark samples was significantly higher than of wood samples. For *C. obtusa*, degradation peaks were much less pronounced and at higher temperatures for bark samples (around 320 °C) than for wood samples, indicating that a higher activation energy is needed to decompose woody biomass, which could result from more, and different types of, lignin compared to wood [26]. Bark *V. surinamensis* showed the best thermal stability over the studied temperature range.

PCFC tests were also conducted to study fractions' fire reaction. Peak values obtained (pHRR) are similar to those found in the literature for wood [27]. The heat release rates (HRR) versus temperature curves (Fig. 8) confirmed that wood fibers have similar thermal behavior. The only difference between wood fibers was the lower temperature peak T(pHRR) for *C. obtusa*.

Bark samples released markedly less energy than woods, with pHRR equal to 71 W/g (compared to 147 W/g on average for wood fractions) and THR equal to approximately 7 kJ/g (compared to 11.6 kJ/g on average for wood fractions). They also generate more char during their decomposition (750 °C): around 25% char compared to 16.2% on average for

wood fractions. This is desirable as it enhances the fire resistance of materials: carbonaceous char produces less combustible gases. ΔH represents the intrinsic energy of gases released during combustion, and lower values were obtained for bark fractions. The higher quantity of chars formed from bark can explain this result, since chars store high quantities of carbon, which tends to reduce the energy of gases.

Bark fractions thus showed better thermal stability and fire reaction compared to wood, which could originate from higher rates of extractives and/or lignin, which are associated with a high carbon content and result in higher yields of char [25]. The presence of specific chemical components, such as suberin, which contribute to shielding against heat-induced degradation [28] could also contribute to the results.

Fiberboard Manufacturing and Microstructure: The Effect of Wood and Bark Fractions' Morphology

Uniformity of air-laid webs depends on fiber spacing, the proportion of synthetic fibers, and the airflow profile. As a starting point, we based processing parameters on those used in studies of pine, poplar, and eucalyptus fiber fractions of about 2 mm in length [6]. Using the same protocol with the small-sized fractions studied in this work, we observed a severe mass loss of more than 80% during web formation and fiber mats with poor cohesion. Therefore, the processing parameters were adapted. First, air suction was halved from 50 to 25% to limit mass loss due to the aspiration of fine particles. Second, the carding of the fractions was omitted since no fiber tufts could be observed and because the fibers could not be orientated for such small dimensions. However, carding of the synthetic fibers was repeated 2 times, to facilitate mixing with lignocellulosic fibers and improve mat cohesion. Finally, the stretching ratio was decreased from 2 to 0.5 in order to increase mat compaction and improve its cohesion. Thanks to these adjustments, average mass losses were greatly reduced (Table 4), but still higher than the values reported [18] for hardwood species (25% for poplar and 28% for eucalyptus). Even after optimization, the high ratio of fine particles present in the studied fractions remains an issue: suction of the smallest particles leads to high mass losses.

Table 4 Processing parameters and key characteristics of the fiberboards produced from each wood/bark fraction

Material	N	Synthetic fibers rate (%)	Mass (g)	Loss rate (%)	Thickness (mm)	Apparent density (kg/m ³)
<i>D. guianensis</i>	4	10	401	53	22.0	203
<i>S. rubra</i>	4	10	500	38	25.5	267
<i>C. obtusa</i>	5	8	382	43	30.0	166
Bark <i>C. obtusa</i>	3	17	200	72	18.0	141
Bark <i>V. surinamensis</i>	3	15	293	66	15.2	202

N number of panels produced, *Mass* average mass per panel sample, *Loss rate* fraction mass loss rate during mat forming processes, *Synthetic fibers rate* amount of synthetic fibers added to the fractions to achieve satisfactory mat cohesion, optimized for each species, *Thickness* final thickness of the mat after consolidation, *Apparent density* bulk density of the mat at 20 °C, 65% RH. All fiberboards were consolidated at 135 °C

As a result, a higher ratio of synthetic fibers was needed to reach satisfying mat cohesion (from 8 to 17% for Bark *C. obtusa*, compared to 6% for the reference pine fibers of 2 mm length, according to Vignon [18]). Here, a strong negative correlation (Pearson's $r = -0.99$; p -value < 0.01) was found between fiber particle size (d_{50}) and the amount of synthetic fibers needed to reach satisfying cohesion (Fig. 9a). As a result, the bark fiber-based fiberboards were composed of a higher proportion of synthetic fibers and were more compact with thicknesses from 15 to 18 mm (Table 4 and Fig. 10), which is expected to lower insulation performances. *C.*

obtusa and *S. rubra* fiberboards were the easiest to manufacture and resulted in the thickest mats (up to 30 mm) produced in this study (Table 4 and Fig. 10). Comparing the morphological features of the fibers and the resulting thickness of the mats, we found a significant positive correlation (Pearson's $r = -0.83$; p -value < 0.01), with greater fiber aspect ratio leading to better cohesion and thus lower fiberboard thickness (Fig. 9b). Previous research indicates that increasing fiber length enhances the mechanical performances of paper and bio-composite materials as it promotes

Fig. 9 Influence of fiber size (a) and aspect ratio (b) on the processing of fiberboards in terms of proportion of synthetic fibers and final thickness. Points represent wood fiberboards (red: *D. guianensis*; black: *S. rubra*; blue: *C. obtusa*) and triangles bark fiberboards (blue: Bark *C. obtusa*; green: Bark *V. surinamensis*); r : correlation coefficient of Pearson; ** p -value < 0.01

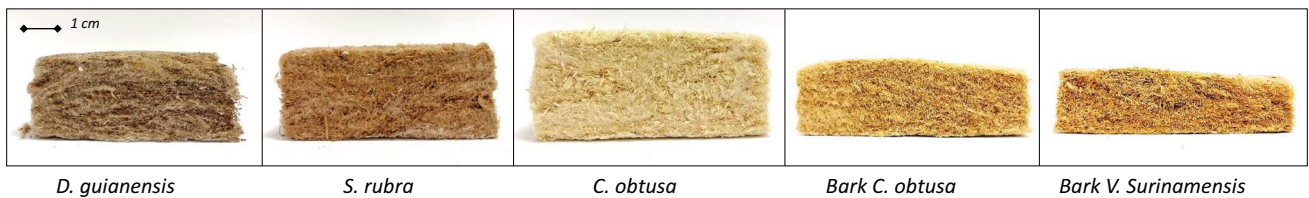
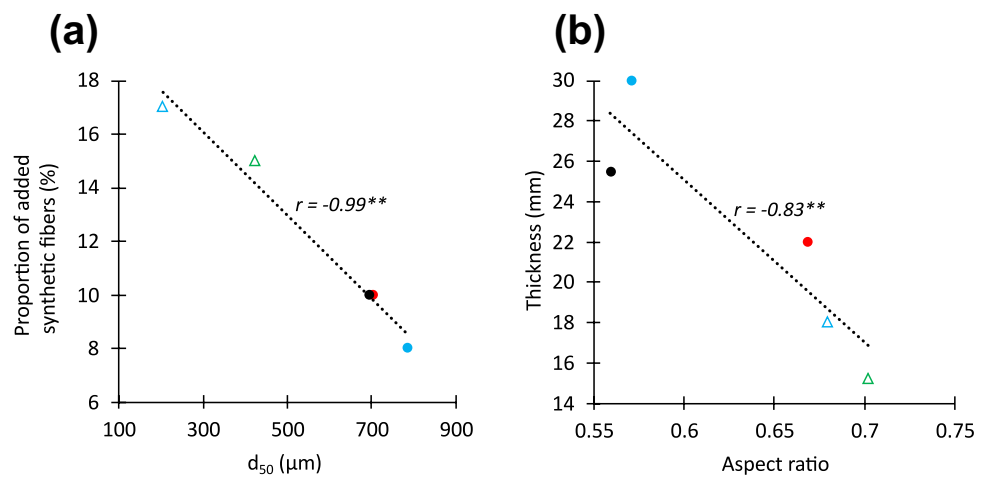


Fig. 10 Final aspect of the produced insulation fiberboards from each wood/bark fraction

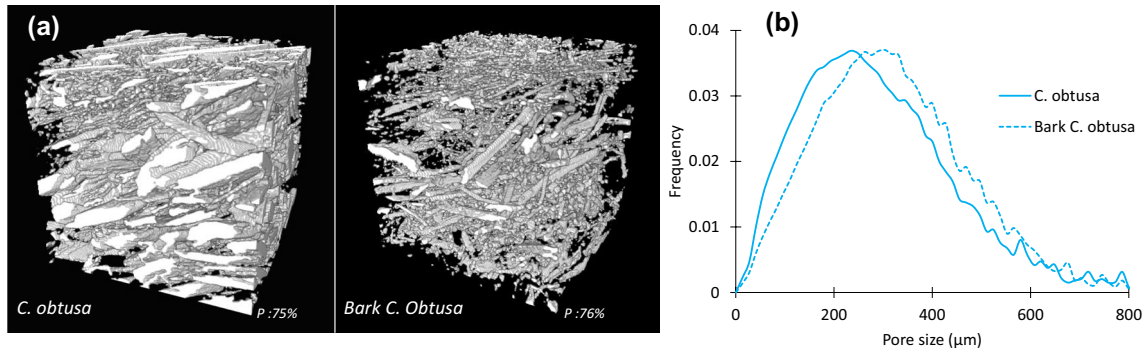


Fig. 11 **a** 3D volume elements reconstructed from successive X-ray projections, corresponding to the fiberboards of *C. obtusa* (left) and Bark *C. obtusa* (right); *P*: porosity. **b** Pore size distribution computed from the 3D volume elements

fiber inter-bonding, allowing the formation of a cohesive 3D interlocked fiber network [29, 30].

In summary, besides controlling the amount of fine particles, our results also showed that fiber aspect ratio is a key morphological parameter to be considered to enhance the manufacturing and structuration of fiberboards. Besides morphological properties, the chemical composition of the fractions can also influence the microstructuration of the fiberboards during the heating phase and their adherence to synthetic fibers. The chemical reactions and physical consolidation of the fibers induced by heat and pressure can favor self-bonding reactions in binderless fiberboards [31]. In particular, the softened surface lignin molecules of fibers might fuse and form covalent bonds [32]. In the case of the wood and bark fractions studied here, a detailed analysis of their chemical composition will be necessary to better understand the mechanism at play.

The internal microstructure of the fiberboards produced from the two most contrasted fiber fractions in terms of morphological characteristics, i.e., *C. obtusa* (d_{50} : 0.79 mm; Aspect ratio: 0.571) and Bark *C. obtusa* (d_{50} : 0.21 mm; Aspect ratio: 0.793), was studied using X-ray tomography. Visual observations of X-ray tomography images confirmed that a larger share of large-sized and elongated particles can be observed in *C. obtusa* compared to Bark *C. obtusa*. As a result, these two fiberboards were characterized by different apparent densities (166 kg/m^3 and 141 kg/m^3 for *C. obtusa* and 141 kg/m^3 for Bark *C. obtusa* fiberboards, Table 4). However, probably because of the large share of FPs observed in bark fractions, pore size distributions were similar for both fiberboards, with slightly larger pores observed for Bark *C. obtusa* (average distance between two fibers of $323 \mu\text{m}$ compared to $297 \mu\text{m}$ for wood; total porosity: 75% for wood and 76% for bark) (Fig. 11b).

Evaluation of Fiberboard Performance

Insulation Performance

The thermal conductivity of the fiberboards produced in this study is illustrated in Fig. 12, and compared to the commercial reference fiberboards made from pinewood (*Pinus pinaster*) (orange squares on Fig. 12). For the commercial reference, testing samples of varying densities has shown an optimal density of 60 kg/m^3 to achieve lowest thermal conductivity of 0.045 W/m/K (Vignon, 2020). Because of the small size and high aspect ratio of the fibers used in this work, mat cohesion required increased compaction of the fiberboards. As a result, the density of the fiberboards produced in this study ranged between 141.9 and 267.7 kg/m^3 , corresponding to the upper range of the pinewood reference curve. Therefore, our results might not cover the optimum thermal conductivity/fiberboard density ratio obtainable for each fraction. Nevertheless, without any optimization of the fiber morphological characteristics, the fiberboards produced in this study from tropical wood and bark have a thermal conductivity close to or even lower than those

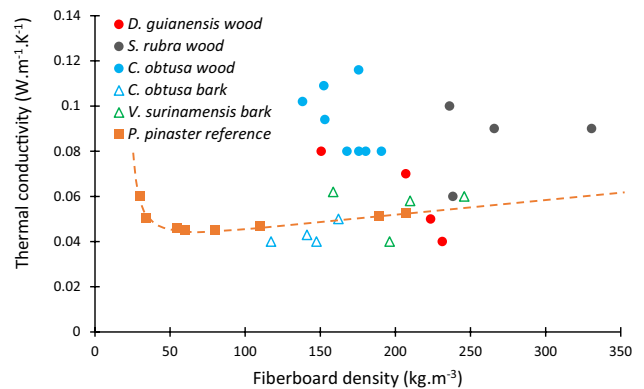


Fig. 12 Evolution of the thermal conductivity of fiberboards as a function of their density at 12% moisture content

reported for the commercial reference in the same density range (Fig. 12). But it should also be pointed out that different defibering conditions were used for the pine commercial reference and the tropical fibers used in this work. Still, these results are promising and it is reasonable to assume that highly efficient insulating material could be produced from these resources with further optimization of fiber preparation and fiberboard manufacturing.

However, results varied depending on the fibers used. *S. rubra* and *D. guianensis* wood fiberboards offer medium to high thermal conductivities, respectively, ranging from 0.04 to 0.1 W/m/K. High, scattered thermal conductivity values were recorded for these samples, which might originate from the natural chemical and structural variability in trees already reported by several authors for these two species [33–35]. Consequent natural variability in fractions produced must be taken into account in order to evaluate realistic final properties of the fiberboards manufactured from residual fibers. On the contrary, fiberboards produced from bark fractions showed the best and less scattered results, with insulating performances higher than the commercial reference in the same density range. Belley [36] suggested that mat density, fiber size and pore sizes mostly influence the thermal conductivity of fiber mats. Here, the small-sized bark particles could contribute to the creation of a specific pore network, thus promoting better insulation performance. For *C. obtusa*, a clear difference can be observed between fiberboards produced from wood or bark fractions. Despite easy processing and promising microstructuration, fiberboards produced from *C. obtusa* wood fibers showed the poorest thermal performance, i.e., high thermal conductivity around 0.1 W/m/K.

Since no glue was used during fiberboard production (synthetic fibers should not influence the material's thermal properties), and samples were stabilized to the same water content prior testing, thermal conductivity should have depended only on the intrinsic properties of natural fibers used, the resulting microstructure and overall porosity and pore size distribution of the fiberboards [7, 37]. X-ray tomography confirmed that pore size distribution and porosity were similar for fiberboards made from wood and bark fibers of *C. obtusa*, with only slightly larger pores in bark-based fiberboards. This suggests that the good thermal conductivity of fiberboards produced from bark fibers could be related to the good intrinsic thermal properties of the fibers. This assumption seems consistent with the fact that bark naturally has protecting functions for the tree, including thermal insulation to resist climate variations (T °C and RH). But further investigation is needed to better understand the insulating performance of bark-based fiberboards in relation to their microstructure.

In summary, barks fibers from *C. obtusa* and *V. surinamensis* appear to be promising resources for the production of insulation fiberboards, and wood fibers from *S. rubra* and *D. guianensis* show encouraging results. Improving the milling process to better control particle size and aspect ratio and resulting fiberboards microstructure could produce even better insulating performance. Our results also raised an important point regarding fraction selection. We observed that besides correct processing of the mats, the microporous network structure of the mat and the specific properties of the selected fibers are critical for insulating performance.

Water Affinity

Affinity to water at high RH and behavior over several RH cycles is a key parameter of our fiberboards' quality as insulating materials, given that they are intended to be used in the humid environment (58% to 73% RH) of French Guiana for outdoor use, degradation by wood-decaying fungi occurs at high humidity levels.

Figure 13 displays the sorption isotherms obtained for each fiberboard, where the stabilized values of moisture content (EMC) are represented along five different RH stages for wood (solid lines) and bark fibers (dotted lines). The curves overlap at low RH stages but diverge at higher RH. Fiberboards produced from wood fibers showed lower maximal water uptake compared to the pinewood reference (at 90% RH: EMC = 11.84% for *S. rubra*, 13.02% for *D. guianensis*, 14.02% for *C. obtusa*, and 18% for the pinewood reference). Fiberboards produced from bark showed the highest values of water uptake (at 90% RH: EMC = 18.70% for Bark *C. obtusa* and 15.15% for Bark *V. surinamensis*). Fiberboards made from Bark *C. obtusa* behaved similarly to the reference pinewood fiberboard with EMC increasing significantly at

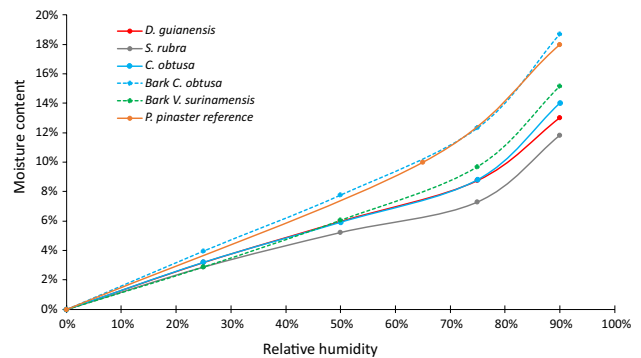


Fig. 13 Sorption isotherms obtained for each fiberboard sample, using DVS. Wood species = solid lines, bark species = dotted lines. The influence of RH on moisture content is represented at each RH stage. Equilibrium moisture content values (EMC) consist of the stabilized quantity of water sorbed by the samples after reaching the equilibrium criteria of $dm/dt < 0.001\%$

low RH stages (being on average more than 30% higher than other samples at 50% RH). Like the commercial pinewood reference, fiberboards produced from Bark *C. obtusa* thus showed a marked affinity to water compared to those produced from other studied species, which might be due to a high content of hemicellulose or low content of extractives.

Given that humidity can fluctuate in French Guiana between day (59% RH at 11:00 am) and night (92% RH at 05:00 am), the kinetics of moisture sorption, as well as the stabilized values (EMC), are relevant. The specific mass stabilization time (SMST, corresponding to the time per unit of mass necessary to reach a mass equilibrium after a change in RH from 75 to 90%) is reported for each sample in Fig. 14. For fiberboards made from wood fibers, variations in SMST could be influenced by variations in fiber density and extractives content (see Table 1). Sorption mechanisms could be influenced by the hydrophilicity of extractives and fiber cell wall microporosity, increasing or decreasing accessibility to sorption sites [38, 39].

Compared to wood fibers, bark fibers (i) absorbed more water at high RH (Fig. 13) but (ii) need a longer time to reach saturation (highest values of SMST). Because of their strong affinity for water, the moisture content of the bark fiberboards might fluctuate in the range favorable for fungal degradation, highlighting the need to investigate further their natural durability in service-use conditions. However, to protect the tree against pests and diseases, bark generally contains more extractives than wood and should be naturally durable. Morris et al. [40] reported good natural durability for a board material made from pressed spruce bark with no additives. In oak, the inhibiting effect of tannins and suberin could make bark more resistant to fungal growth than wood [41]. Bark extracts are even being considered for developing new bio-based preservative treatments to improve the biological resistance of wood [42]. We propose that fiberboards produced from bark fibers might better regulate humidity

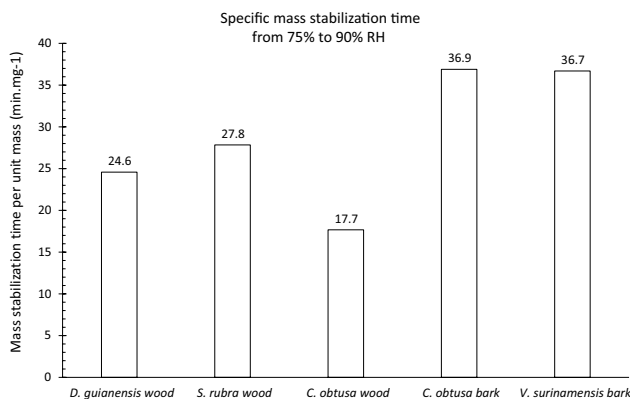


Fig. 14 Average specific mass stabilization time (SMST), corresponding to the time per unit of mass necessary to reach mass equilibrium after RH variation from 75 to 90%

by acting as water buffers since water sorption kinetics are slower compared to wood.

These hypotheses must be verified through long-term and RH cycling experiments. Testing our produced fiberboards in real service-use conditions would enable assessment of (i) their durability and (ii) their insulating performance under fluctuating humidity conditions.

Conclusion

This study was a first step in evaluating the potential of Guyanese waste fibers for the production of insulation fiberboards. Wood residues from two of the most common local commercial species (*D. guianensis* and *S. rubra*) and from an abundant fast-growing species (*C. obtusa*), and bark fibers of interest (Bark *C. obtusa* and Bark *V. surinamensis*), were selected and harvested to manufacture bio-based insulation fiberboards. Fiberboards were produced from milled fiber fractions using an environmentally low impact process using the self-bonding properties of the fibers and a small fraction of synthetic fibers.

Morphological analysis of the milled fractions highlighted the need for an optimization of the milling process to achieve suitable fiber/particle size and shape and adjustments were made. Processing parameters were optimized to limit mass losses and favor mat cohesion. Our results showed that fiber shape is a key morphological parameter to be considered for fiberboard manufacturing, influencing self-bonding of the fibers and improving fiberboard cohesion. In addition to processing parameter optimization, the specific properties of the selected fibers are likely to greatly influence fiberboard performance.

Despite no optimization of the fraction dimension and fiberboard densities, the fiberboards made from tropical wood and bark residues displayed low thermal conductivity. In some cases, fiberboard performance was comparable to the commercial reference. Results obtained for fiberboards produced from bark fractions of *C. obtusa* and *V. surinamensis* and wood fractions of *S. rubra* and *D. guianensis* are encouraging. While bark fiberboards displayed the best resistance to thermal degradation and fire reaction, two parameters of interest for building applications, they were also characterized by higher affinity to water compared to wood fiberboards, showing the highest water uptake at 90% RH. However, bark fiberboards' slow stabilization to reach equilibrium moisture content might be of interest for humidity regulation.

Future in-situ, long-term RH cycling testing will better characterize the insulation performance of our fiberboards. Temperature and moisture content, and their variation, are important parameters affecting thermal properties of wood and wood-based materials. New quantitative data are

required to assess thermal conductivity and durability of insulation fiberboards in real conditions of use. The authors are currently conducting studies in the potential use of natural wood extractives to develop bio-impregnation treatments to enhance the natural durability of the fibers prior to fiberboards manufacturing.

In conclusion, we were able to produce insulation fiberboards from tropical residues comparable with the commercial reference, paving the way for promising future research.

Acknowledgements This research project has been financially supported by a PEPS CNRS-INSIS grant. The authors are grateful to the French National Research Agency (ANR) for its financial support through the Xylomat project, Equipex XYLOFOREST (ANR-10-EQPX-16). The authors thank Romain Lehnebach and Leopold Doumerc for providing bark material. The authors thank the PLANET facility (<https://doi.org/10.15454/1.5572338990609338E12>) run by the IATE joint research unit for its process experiment supports. The authors thank Sophie Bezaud (student at Bordeaux Sciences Agronomique) and Doriane Beuseroy, Amanda Ribas Leão and Frédéric Pécot (students at the Ecole Supérieure du Bois engineering school) for their contributions to the experimental part.

Author Contributions JB contributed to the study conception and design. Material preparation, data collection and analysis were performed by JB, JM, CD and RS. The first draft of the manuscript was written by JB and all authors commented on previous versions of the manuscript. All authors read and approved the final manuscript.

Funding This research project has been financially supported by a PEPS CNRS-INSIS grant. The authors are grateful to the French National Research Agency (ANR) for its financial support through the Xylomat project, Equipex XYLOFOREST (ANR-10-EQPX-16).

Data Availability The datasets generated during and/or analyzed during the current study are available in the “Guyavalofibres” repository, <https://doi.org/10.18167/DVNI/KVNAQ6>.

Declarations

Competing interests The authors have no relevant financial or non-financial interests to disclose.

References

1. Guyane, D.: Quels besoins en logements en Guyane pour les 10 prochaines années? (2017)
2. Hobballah, M.H., Ndiaye, A., Michaud, F., Irle, M.: Formulating preliminary design optimization problems using expert knowledge: application to wood-based insulating materials. *Expert Syst. Appl.* **92**, 95–105 (2018). <https://doi.org/10.1016/j.eswa.2017.09.035>
3. Schiavoni, S., D’Alessandro, F., Bianchi, F., Asdrubali, F.: Insulation materials for the building sector: A review and comparative analysis. *Renew. Sustain. Energy Rev.* **62**, 988–1011 (2016)
4. Latif, E., Lawrence, R.M.H., Shea, A.D., Walker, P.: An experimental investigation into the comparative hygrothermal performance of wall panels incorporating wood fibre, mineral wool and hemp-lime. *Energy Build.* **165**, 76–91 (2018). <https://doi.org/10.1016/J.ENBUILD.2018.01.028>
5. Porter, M., Yu, J.: Crystallization kinetics of poly(3-hydroxybutyrate) granules in different environmental conditions. *J. Biomater. Nanobiotechnol.* **02**, 301–310 (2011). <https://doi.org/10.4236/jbnb.2011.23037>
6. Vignon, P., Hobballah, H.M., Moreau, J., Delisée, C., Irle, M.: Optimization of the thermal properties of wood fiber-based insulating materials. In: *Hygrothermal performance of buildings and their materials*, Joint Conference: COST Action FP1303 & DURAWOOD Project, Poznan, Poland (2016)
7. Sonderegger, W.U.: Experimental and theoretical investigations on the heat and water transport in wood and wood-based materials. *J. Biomater. Nanobiotechnol.* (2011). <https://doi.org/10.3929/ethz-a-006532317>
8. Lehnebach, R., Alméras, T., Clair, B.: How does bark contribution to postural control change during tree ontogeny? A study of six Amazonian tree species. *J. Exp. Bot.* **71**, 2641–2649 (2020). <https://doi.org/10.1093/jxb/eraa070>
9. Gérard, J., Guibal, D., Cerre, J. C., & Paradis, S. (2016). *Atlas des bois tropicaux: caractéristiques technologiques et utilisations*. Editions Quae
10. Gerard, J., Paradis, S., & Thibaut, B. (2019). CIRAD wood chemical composition database
11. Vignon, P., Hobballah, M.H., Tran, H., Moreau, J., Delisée, C., Lecourt, M., Belalia, R., Sanguina, T.: Thermal insulating materials made up of poplar wood fibres. In: *2nd Conference on Engineered Wood Products based on Poplar/Willow Wood CEWPPW2*, Leon (2016)
12. Mayer-Laigle, C., Rajaonarivony, R., Blanc, N., Rouau, X.: Comminution of dry lignocellulosic biomass: Part II. Technologies, improvement of milling performances, and security issues. *Bioengineering* **5**, 50 (2018). <https://doi.org/10.3390/bioengineering5030050>
13. Hill, C.A.S., Norton, A.J., Newman, G.: The water vapour sorption properties of Sitka spruce determined using a dynamic vapour sorption apparatus. *Wood Sci. Technol.* **44**, 497–514 (2010). <https://doi.org/10.1007/s00226-010-0305-y>
14. Engelund, E.T., Klamer, M., Venås, M.: Acquisition of sorption isotherms for modified woods by the use of dynamic vapour sorption instrumentation: principles and practice. In: *41st Annual Meeting of International Research Group (IRG) on Wood Protection*, Biarritz, France, 9–13 May 2010. (2010)
15. David, G.: *Eco-conversion de résidus lignocellulosiques de l’agriculture en matériaux composites durables à matrice biopolyester*. Springer, New York (2019)
16. Rajaonarivony, K., Rouau, X., Lampoh, K., Delenne, J.Y., Mayer-Laigle, C.: Fine comminution of pine bark: how does mechanical loading influence particles properties and milling efficiency? *Bioengineering* (2019). <https://doi.org/10.3390/bioengineering6040102>
17. Maharani, R., Yutaka, T., Yajima, T., Minoru, T.: Scrutiny on physical properties of sawdust from tropical commercial wood species: effects of different mills and sawdust’s particle size. *Indones. J. For. Res.* **7**, 20–32 (2010). <https://doi.org/10.20886/jjfr.2010.7.1.20-32>
18. Vignon, P.: Caractérisation et optimisation des propriétés d’isolants thermiques non tissés à base de fibres de bois (2020)
19. Gil, M.V., Casal, D., Pevida, C., Pis, J.J., Rubiera, F.: Thermal behaviour and kinetics of coal/biomass blends during co-combustion. *Bioresour. Technol.* **101**, 5601–5608 (2010). <https://doi.org/10.1016/j.biortech.2010.02.008>
20. Kong, B., Wang, E., Li, Z., Lu, W.E.I.: Study on the feature of electromagnetic radiation under coal oxidation and temperature rise based on multifractal theory. *Fractals* (2019). <https://doi.org/10.1142/S0218348X19500385>
21. Cai, P., Nie, W., Chen, D., Yang, S., Liu, Z.: Effect of air flow-rate on pollutant dispersion pattern of coal dust particles at fully

- mechanized mining face based on numerical simulation. *Fuel* **239**, 623–635 (2019). <https://doi.org/10.1016/j.fuel.2018.11.030>
22. Cheng, K., Winter, W.T., Stipanovic, A.J.: A modulated-TGA approach to the kinetics of lignocellulosic biomass pyrolysis/combustion. *Polym. Degrad. Stab.* **97**, 1606–1615 (2012). <https://doi.org/10.1016/j.polymdegradstab.2012.06.027>
 23. Dorez, G., Ferry, L., Sonnier, R., Taguet, A., Lopez-Cuesta, J.M.: Effect of cellulose, hemicellulose and lignin contents on pyrolysis and combustion of natural fibers. *J. Anal. Appl. Pyrolysis.* **107**, 323–331 (2014). <https://doi.org/10.1016/j.jaap.2014.03.017>
 24. López-Beceiro, J., Díaz-Díaz, A.M., Álvarez-García, A., Tarrío-Saavedra, J., Naya, S., Artiaga, R.: The complexity of lignin thermal degradation in the isothermal context. *Process.* **9**, 1154 (2021). <https://doi.org/10.3390/PR9071154>
 25. Di Blasi, C.: Combustion and gasification rates of lignocellulosic chars. (2009)
 26. Burhenne, L., Messmer, J., Aicher, T., Laborie, M.P.: The effect of the biomass components lignin, cellulose and hemicellulose on TGA and fixed bed pyrolysis. *J. Anal. Appl. Pyrolysis.* **101**, 177–184 (2013). <https://doi.org/10.1016/J.JAAP.2013.01.012>
 27. Haurie, L., Giraldo, M.P., Lacasta, A.M., Montón, J., Sonnier, R.: Influence of different parameters in the fire behaviour of seven hardwood species. *Fire Saf. J.* **107**, 193–201 (2019). <https://doi.org/10.1016/j.firesaf.2018.08.002>
 28. Şen, A., Van den Bulcke, J., Defoirdt, N., Van Acker, J., Pereira, H.: Thermal behaviour of cork and cork components. *Thermochim. Acta.* **582**, 94–100 (2014). <https://doi.org/10.1016/j.tca.2014.03.007>
 29. Taipale, T., Österberg, M., Nykänen, A., Ruokolainen, J., Laine, J.: Effect of microfibrillated cellulose and fines on the drainage of kraft pulp suspension and paper strength. *Cellulose* **17**, 1005–1020 (2010). <https://doi.org/10.1007/s10570-010-9431-9>
 30. Stark, N.M.: Effects of wood fiber characteristics on mechanical properties of wood/polypropylene composites. (2003)
 31. Hashim, R., Nadhari, W.N.A.W., Sulaiman, O., Kawamura, F., Hiziroglu, S., Sato, M., Sugimoto, T., Seng, T.G., Tanaka, R.: Characterization of raw materials and manufactured binderless particleboard from oil palm biomass. *Mater. Des.* **32**, 246–254 (2011). <https://doi.org/10.1016/j.matdes.2010.05.059>
 32. Börcsök, Z., Pásztor, Z.: The role of lignin in wood working processes using elevated temperatures: an abbreviated literature survey. *Eur. J. Wood Wood Prod.* **79**, 511–526 (2020). <https://doi.org/10.1007/S00107-020-01637-3>
 33. Lehnebach, R., Bossu, J., Va, S., Morel, H., Amusant, N., Nicolini, E., Beauchêne, J.: Wood density variations of legume trees in French Guiana along the shade tolerance continuum: heartwood effects on radial patterns and gradients. *Forests* **10**, 80 (2019). <https://doi.org/10.3390/f10020080>
 34. Flora, C.: Origine et prédiction de la variabilité de la durabilité naturelle chez *Dicorynia guianensis* Amsh, Guyane (2018)
 35. Houël, E., Rodrigues, A.M.S., Nicolini, E.-A., Ngwete, O., Duplais, C., Stien, D., Amusant, N.: Natural durability of *Sextonia rubra*, an Amazonian tree species: description and origin (2017)
 36. Belley, D.: Détermination des propriétés de transfert de chaleur et de masse des panneaux de fibres de bois. Springer, New York (2009)
 37. Suleiman, B.M., Larfeldt, J., Leckner, B., Gustavsson, M.: Thermal conductivity and diffusivity of wood. *Wood Sci. Technol.* **33**, 465–473 (1999). <https://doi.org/10.1007/s002260050130>
 38. Wangaard, F.F., Granados, L.A.: The effect of extractives on water-vapor sorption by wood. *Wood Sci. Technol.* **1**, 253–277 (1967). <https://doi.org/10.1007/BF00349758>
 39. Choong, E.T., Achmadi, S.S.: Effect of extractives on moisture sorption and shrinkage in tropical woods. *Wood Fiber Sci.* **1**, 185–196 (1991)
 40. Morris, P.L., Grace, J.K., Troughton, G.E.: Preliminary indications of the natural durability of spruce bark board. (1999)
 41. Vane, C.H., Drage, T.C., Snape, C.E.: Bark decay by the white-rot fungus *Lentinula edodes*: polysaccharide loss, lignin resistance and the unmasking of suberin. *Int. Biodeterior. Biodegrad.* **57**, 14–23 (2006). <https://doi.org/10.1016/j.ibiod.2005.10.004>
 42. Lajnef, L., Caceres, I., Trinsoutrot, P., Charrier-El Bouhtoury, F., Ayed, N., Charrier, B.: Effect of *Punica granatum* peel and *Melia azedarach* bark extracts on durability of European beech and maritime pine. *Eur. J. Wood Wood Prod.* **76**, 1725–1735 (2018). <https://doi.org/10.1007/s00107-018-1340-x>

Publisher's Note Springer Nature remains neutral with regard to jurisdictional claims in published maps and institutional affiliations.

Springer Nature or its licensor (e.g. a society or other partner) holds exclusive rights to this article under a publishing agreement with the author(s) or other rightsholder(s); author self-archiving of the accepted manuscript version of this article is solely governed by the terms of such publishing agreement and applicable law.

Authors and Affiliations

Julie Bossu¹  · Jérôme Moreau^{2,3} · Christine Delisée³ · Nicolas Le Moigne⁶ · Stéphane Corn⁷ · Rodolphe Sonnier⁶ · Amandine Viretto⁵ · Jacques Beauchêne⁴ · Bruno Clair⁸

Terms and Conditions

Springer Nature journal content, brought to you courtesy of Springer Nature Customer Service Center GmbH (“Springer Nature”).

Springer Nature supports a reasonable amount of sharing of research papers by authors, subscribers and authorised users (“Users”), for small-scale personal, non-commercial use provided that all copyright, trade and service marks and other proprietary notices are maintained. By accessing, sharing, receiving or otherwise using the Springer Nature journal content you agree to these terms of use (“Terms”). For these purposes, Springer Nature considers academic use (by researchers and students) to be non-commercial.

These Terms are supplementary and will apply in addition to any applicable website terms and conditions, a relevant site licence or a personal subscription. These Terms will prevail over any conflict or ambiguity with regards to the relevant terms, a site licence or a personal subscription (to the extent of the conflict or ambiguity only). For Creative Commons-licensed articles, the terms of the Creative Commons license used will apply.

We collect and use personal data to provide access to the Springer Nature journal content. We may also use these personal data internally within ResearchGate and Springer Nature and as agreed share it, in an anonymised way, for purposes of tracking, analysis and reporting. We will not otherwise disclose your personal data outside the ResearchGate or the Springer Nature group of companies unless we have your permission as detailed in the Privacy Policy.

While Users may use the Springer Nature journal content for small scale, personal non-commercial use, it is important to note that Users may not:

1. use such content for the purpose of providing other users with access on a regular or large scale basis or as a means to circumvent access control;
2. use such content where to do so would be considered a criminal or statutory offence in any jurisdiction, or gives rise to civil liability, or is otherwise unlawful;
3. falsely or misleadingly imply or suggest endorsement, approval, sponsorship, or association unless explicitly agreed to by Springer Nature in writing;
4. use bots or other automated methods to access the content or redirect messages
5. override any security feature or exclusionary protocol; or
6. share the content in order to create substitute for Springer Nature products or services or a systematic database of Springer Nature journal content.

In line with the restriction against commercial use, Springer Nature does not permit the creation of a product or service that creates revenue, royalties, rent or income from our content or its inclusion as part of a paid for service or for other commercial gain. Springer Nature journal content cannot be used for inter-library loans and librarians may not upload Springer Nature journal content on a large scale into their, or any other, institutional repository.

These terms of use are reviewed regularly and may be amended at any time. Springer Nature is not obligated to publish any information or content on this website and may remove it or features or functionality at our sole discretion, at any time with or without notice. Springer Nature may revoke this licence to you at any time and remove access to any copies of the Springer Nature journal content which have been saved.

To the fullest extent permitted by law, Springer Nature makes no warranties, representations or guarantees to Users, either express or implied with respect to the Springer nature journal content and all parties disclaim and waive any implied warranties or warranties imposed by law, including merchantability or fitness for any particular purpose.

Please note that these rights do not automatically extend to content, data or other material published by Springer Nature that may be licensed from third parties.

If you would like to use or distribute our Springer Nature journal content to a wider audience or on a regular basis or in any other manner not expressly permitted by these Terms, please contact Springer Nature at

onlineservice@springernature.com